ARTICLE NO. 80-4035

J80-094

0001
0005

Analysis of Two-Dimensional Incompressible Flows by a Subsurface Panel Method

Jack Moran,* Kevin Cole,† and David Wahl‡
University of Minnesota, Minneapolis, Minn.

A new approach to panel methods is explored for two-dimensional steady incompressible flows. The method uses linear distributions of sources and vortices on straight-line panels, but satisfies boundary conditions on the actual body surface, at nodes that are also end points of the panels. The result is continuity in body-surface velocity distribution, without recourse to numerical quadrature for the velocity influence coefficients. The method is unusually sensitive to the distribution of the nodes. For example, it almost always fails to give acceptable results when the nodes are distributed randomly. However, the continuity of the velocity distribution makes possible a unique node redistribution scheme, which may be iterated to give accurate results reliably.

Background

PANEL methods are now widely used for calculating linear potential flows past aerodynamic bodies. The steps involved in setting up a panel method are as follows:

1) Represent the perturbation potential by a distribution of sources, doublets, and/or vortices of unknown strength over the body surface and its wake.
2) Approximate the body and wake surfaces by the union of panels of relatively simple geometry.
3) Parameterize the singularity strength on the panels; e.g., represent it by a polynomial of degree two or less.
4) For each unknown parameter in the representation of the singularity strength, demand that the potential and/or velocity field satisfy an appropriate boundary condition at some control point.
5) Solve the resulting system of linear algebraic equations for the parameters underlying the singularity strength.

Once these steps are completed, the velocity and potential may be evaluated anywhere in the flow by summing contributions from the individual panels.

Almost invariably, approximations made in the formulation of panel methods lead to singularities at the panel boundaries, and so restrict the usable output of the methods to points near the panel center. This is certainly the case if the panels are plane or piecewise plane. However, even when curved panels are used, spurious singularities sometimes result.[1-3] The integrals which give the potential and velocity fields due to the singularity distributions on the panels cannot be evaluated in closed form unless they are approximated through series expansion by integrals over plane or piecewise-plane surfaces. In effect, the source, doublet, or vortex distribution over a curved surface is replaced by a series of multipole distributions over a plane surface. At the panel edges, each term of the expansion is even more singular than the one preceding.

Received May 7, 1979; revision received Aug. 27, 1979.

Index categories: Computational Methods; Aerodynamics.

*Associate Professor, Dept. of Aerospace Engineering and Mechanics.

†Graduate Student, Dept. of Aerospace Engineering and Mechanics.

‡National Science Foundation Summer Intern, Dept. of Aerospace Engineering and Mechanics.

A related problem of existing panel methods, at least in three-dimensional situations, is the rather complicated way in which they approximate the body surface. Since panel edges are not available as control points, there is generally just one control point per panel, and thus (approximately) one unknown per panel as well. Quadrilateral panels are therefore preferred to triangles, since the latter would double the number of unknowns for a given number of points at which data on the body shape are specified. However, to avoid numerical quadrature, the surfaces on which the singularities are distributed should be plane, and a curved three-dimensional surface cannot be approximated by a continuous system of plane quadrilaterals. Some methods simply allow gaps between neighboring panel edges; others use a piecewise-planar quadrilateral (four triangles surrounding a planar parallelogram whose corners are the midpoints of the sides of the quadrilateral).

The use of (roughly) one control point per panel also complicates the parameterization of the singularity strength. Recent methods are based on quadratic doublet distributions. In order to specify the ten coefficients of the quadratics without creating discontinuities at panel or subpanel boundaries, one method uses a singularity spline based on a least-squares fit of the quadratic in one panel to the doublet strength in twenty surrounding panels.

A more local support for the singularity splines is desirable for a number of reasons. First, the more local the spline, the easier it is to match the singularity strength at boundaries between distinct networks of singularity distributions (e.g., at wing-body junctions). Also, a wide support suggests that the effective mesh size is much larger than the distance between nodes. Finally, a more local spline would probably simplify and, hence, expedite the analysis.

The objective of the present research, therefore, is to develop a panel method with the following characteristics: 1) the velocity distribution on the body surface should be continuous, even at panel edges; 2) integrals giving the velocity field should be evaluated in closed form; and 3) both the body surface and the singularity strength should be specified by splines of local support. Thus far we have succeeded in implementing a two-dimensional version of a method which promises to meet all three objectives. This paper reports our progress.

Analysis

We want to determine the aerodynamics of an airfoil of specified geometry immersed in a uniform steady incompressible inviscid flow. A general representation of the perturbation velocity potential may be constructed by

distributing sources and vortices over a surface S:

$$\phi_P = \frac{1}{2\pi}\int_S (\sigma_Q \ell n r_{QP} - \gamma_Q \theta_{QP})\,ds \tag{1}$$

Here P is a typical field point, Q a point on S, and r_{QP}, θ_{QP} polar coordinates of P relative to Q. The quantities σ_Q and γ_Q are the strengths per unit length of the source and vortex distributions, respectively, at Q.

For any given source and vortex distributions, Eq. (1) satisfies the conditions of continuity and irrotationality and also the boundary condition at infinity. To make Eq. (1) the solution of a particular flow problem, it is only necessary that it also meet the flow-tangency condition on the airfoil surface and the circulation condition.

Before we can proceed further, we must specify the surface S—the "panels" of the method—on which the sources and vortices are distributed. Equation (1) is essentially equivalent to Green's third identity, according to which the potential outside S is representable by a source distribution of strength $\partial\phi/\partial n$ and a doublet distribution of strength ϕ on S. The restrictions on the validity of Eq. (1) are therefore the same as those on Green's third identity; namely, that ϕ is a continuous single-valued solution of Laplace's equation outside the surface S on which the sources and vortices are distributed. A safe choice for the panel surface, therefore, is the surface of the body under study.

However, it is difficult to evaluate the requisite integrals if the panel surface is curved. In the subsurface panel method, therefore, we distribute the sources and vortices on straight-line panels, whose endpoints are nodes on the body surface, as shown in Fig. 1, but continue to satisfy the flow-tangency condition on the actual body surface. This distinction between the panel and body surfaces is consistent with the limits on the validity of Green's identity, provided the flow has an analytic continuation across the body surface to the panels if, as is usually the case, the panels lie within the body. Since the panel surface can be made to approximate the body surface as closely as desired simply by increasing the panel density, this condition is not expected to be overly restrictive. However, it does necessitate the special treatment of (if not exclude from consideration) flows that are truly singular; in particular, flows past bodies with convex corners or sharp edges (aside from edges at which a Kutta condition removes the singularity).

Even with the panel surface S of Eq. (1) specified, the flow tangency and circulation conditions do not determine the source and vortex strengths uniquely. It is possible to specify one of them almost arbitrarily and then to determine the other so that Eq. (1) meets all the conditions it should. A convenient way to supply a closure condition is to specify a fictitious velocity field inside the surface S. In our work, this fictitious field has zero velocity. Then σ and γ are, respectively, the normal and tangential components of the total (not perturbation) velocity on the outside of the panel surface.

In order to discretize the problem, we approximate the source and vortex distributions as linear over each panel. Such distributions may be parameterized in terms of the source and vortex strengths at the vertices of the panels, which in turn equal the velocity components normal and tangential to the panels at their vertices. Since the vertices are also nodes on the body surface, these are components of the total fluid velocity on the body surface.

Specifically, let the jth panel be the straight line between the jth and $(j+1)$th nodes, ℓ_j its length, and ξ the distance from the jth node, as shown in Fig. 2. Then we take

$$\sigma(\xi) = \sigma_0 + (\sigma_\ell - \sigma_0)(\xi/\ell_j),\quad \gamma(\xi) = \gamma_0 + (\gamma_\ell - \gamma_0)(\xi/\ell_j) \tag{2}$$

in which, because the singularity strengths at $\xi = 0$ and ℓ_j are components of the total fluid velocity at the jth and $(j+1)$th nodes, respectively,

$$\begin{pmatrix} \sigma_0 \\ \gamma_0 \end{pmatrix} = [R(\theta_j - \beta_j)] \begin{pmatrix} V_{n_j} \\ V_{t_j} \end{pmatrix}$$

$$\begin{pmatrix} \sigma_\ell \\ \gamma_\ell \end{pmatrix} = [R(\theta_{j+1} - \beta_j)] \begin{pmatrix} V_{n_{j+1}} \\ V_{t_{j+1}} \end{pmatrix} \tag{3}$$

Here V_{n_j} and V_{t_j} are the velocity components normal and tangential to the body surface at the jth node, θ_j the inclination of the body surface at the same point, β_j the inclination of the jth panel, and $[R]$ a rotation matrix:

$$[R(\theta)] = \begin{bmatrix} \cos\theta & \sin\theta \\ -\sin\theta & \cos\theta \end{bmatrix} \tag{4}$$

This parameterization allows us to achieve our first major objective, continuity of the body-surface velocity. The velocity field due to any one panel does blow up at the ends of that panel. However, with our parameterization, the singularities due to neighboring panels cancel exactly, as is shown in the Appendix.

Note, on the other hand, that the source and vortex strengths themselves are not continuous from one panel to the next. The singularity strengths are, as previously pointed out, velocity components normal or tangential to the panel. At a node, the source and vortex strengths on the panels which meet there are components of the same velocity, the local body-surface velocity. But, because panels generally meet at an angle, the components of that velocity normal and tangential to the panels differ, and so, then, do the local source and vortex strengths.

Since V_{n_j} is known at each node from the flow-tangency condition, our unknowns are the nodal tangential velocity components. These we determine by satisfying an integral equation for V_t at each node,

$$V_{t_i} = \frac{1}{2\pi}\int_S [\sigma_Q \hat{t}_i \cdot \nabla_i \ell n r_{Qi} - \gamma_Q \hat{t}_i \cdot \nabla_i \theta_{Qi}]\,ds + V_\infty \cdot \hat{t}_i \tag{5}$$

which is derived by differentiating Eq. (1). Contributions to Eq. (5) from the panels adjacent to the ith node must be subjected to a limiting process, in which the field point approaches the ith node from the outside S; see the Appendix for some of the details.

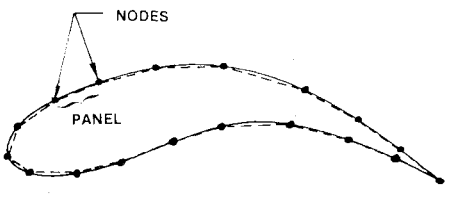

Fig. 1 Subsurface paneling.

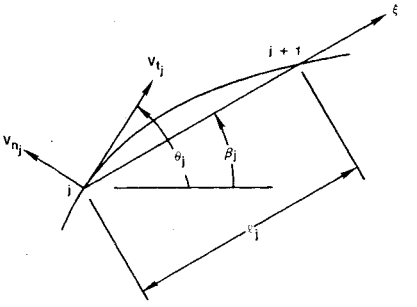

Fig. 2 Nomenclature used in formulas for source and vortex strengths.

An alternative approach is to require the velocity tangential to the body surface to vanish on the inside of each node. Because of the jumps in velocity across the panels, the resultant formula is exactly equivalent to Eq. (5), and we shall refer to Eq. (5) both as an "integral equation for the external tangential velocity" and a "requirement of vanishing internal tangential velocity."

Circulation Condition

For sharp-tailed airfoils, the circulation is fixed by the Kutta condition, that the velocity be finite at the trailing edge. Unless the trailing edge is cusped, this implies that the trailing edge is a stagnation point. Although we can show that, in principle, our solution yields finite velocities at sharp-but-not-cusped trailing edges if, and only if, the flow stagnates there, simply replacing Eq. (5) at the trailing-edge nodes by the stagnation condition

$$V_{t_j} = 0 \text{ at trailing-edge stagnation points} \qquad (6)$$

yielded obviously incorrect results, including pressures higher on the leeward side of the trailing edge than on the windward.

Similarly poor results were obtained when we attempted a variety of alternative circulation conditions, including equation of the tangential velocities at the trailing-edge nodes and requiring the trailing-edge bisector to be a streamline, with such conditions used in place of Eq. (5) at one or both trailing-edge nodes. What such formulations seem to ignore is that the circulation condition is a requirement that the solution must satisfy over and above the integral equation approximated by Eq. (5). In any case, we obtain good results only by solving an overdetermined system comprised of an equation like Eq. (5) for each node and a circulation condition. For bodies with trailing-edge stagnation points, we use Eq. (6) in place of Eq. (5) at the trailing-edge nodes.

For bodies with sharp trailing edges, the circulation condition used is that the velocity component normal to the trailing edge bisector vanishes at a point very close to the trailing edge; specifically, at a distance from the trailing edge of about 10^{-5} times the average length of the two panels adjacent to the trailing edge. For the present case of steady two-dimensional flow, it makes little difference whether this point is inside or outside the airfoil.

The rationale for this form of the circulation condition was the suppression of the trailing-edge singularity which would follow from failure to satisfy the Kutta condition. However, the singularity is only logarithmic, and, as we discoverd by accident, the results change very little if we simply delete the logarithmically near-singular terms in calculating the velocity at the control point near the trailing edge. On the other hand, no logical alternative circulation condition suggested itself. In particular, we cannot simply require tangential velocities at the two trailing-edge nodes to be equal and opposite. This is already accomplsihed, in effect, by setting Eq. (5) or (6) at the two nodes.

Real airfoils—certainly if viscous displacement effects are taken into account—do not have sharp trailing edges. A cutoff trailing edge is usually modeled by hypothesizing a constant-pressure wake to emanate from the edge. Thus we require that the tangential velocities at the nodes on either side of the trailing edge be equal and opposite. The trailing edge is closed by a single panel, on which the velocity is determined solely by requiring the velocity to be continuous at its two nodes, where it is tangential to the main airfoil surfaces. Thus, the trailing-edge panel supports a fairly strong source distribution. Equation (5) is imposed at the trailing-edge nodes, which implies that the internal velocity tangential to the main airfoil surface vanishes at those nodes (as well as all the others).

The various forms of circulation condition for sharp, cusped, and cutoff trailing edges are summarized in Fig. 3, in which the $X'd$ arrows indicate velocity components that are set to zero.

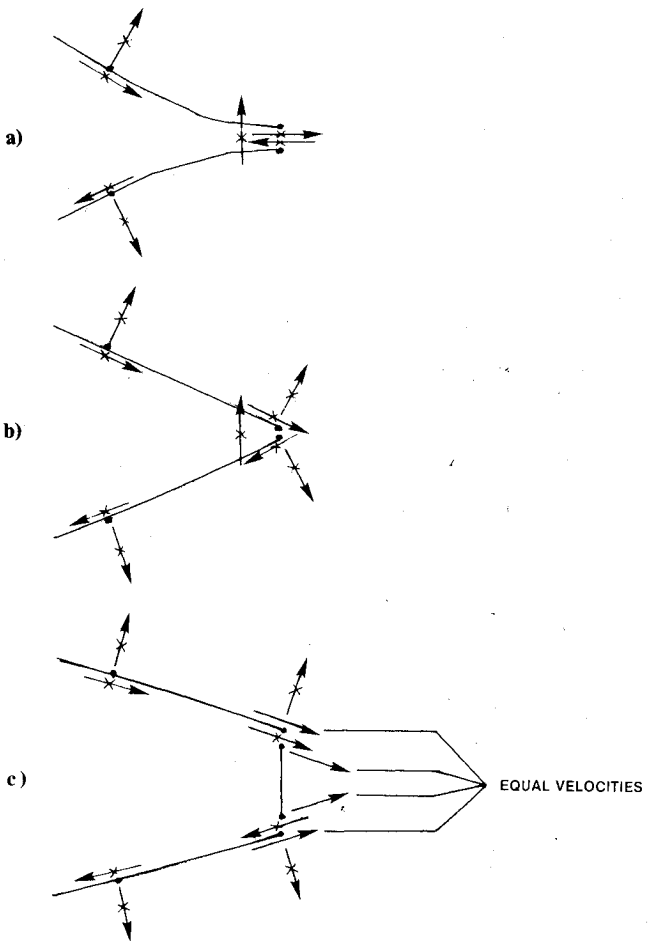

Fig. 3 Summary of boundary conditions imposed at trailing edges of various types: a) cusped, b) sharp but not cusped, and c) cutoff.

As noted above, adding the circulation condition to the system which governs the nodal tangential velocities overdetermines those unknowns. To solve the resultant system, we generally follow Bristow[3] in introducing an extra unknown for each extra equation, namely, a constant error term in all equations like Eq. (5), the constant varying from one element to another in multielement problems. We also provide, in our program, the option of using a least-squares technique. Generally, the two methods give quite comparable results. Bristow's is much cheaper, and so is preferred, but the least-squares method is occasionally more reliable in the node redistribution process to be described below.

Input Requirements

It should be noted that, to obtain a solution for the source and vortex strengths, the only data which must be known about the body shape are its coordinates and slope at the nodes. No assumption or approximation is made concerning the body shape between nodes. Thus, the only approximation made in the analysis is that the source and vortex strengths are assumed to vary linearly with distance along the panels. By invoking the momentum and moment-of-momentum theorems, we reduce force and moment calculations to integrals over the panels rather than over the body surface, so that that part of the calculations, too, is independent of the form of the body surface between nodes. Further, the assumed linearity of the velocity distribution on the panels makes it possible to evaluate in closed form the integrals over the panels required for the force and moment.

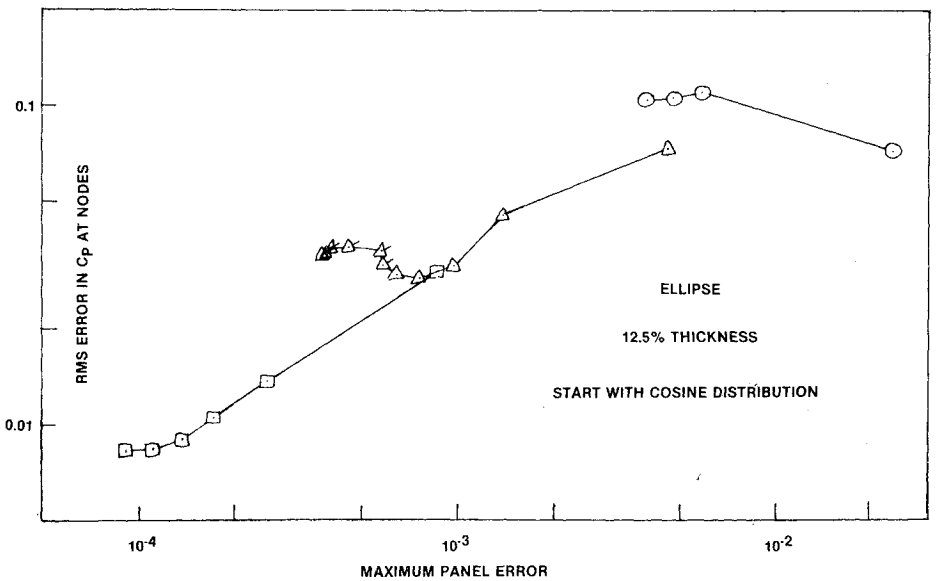

Fig. 4 History of root-mean-squared error during node redistribution process for ellipse of thickness ratio 0.125. Nodes initially distributed by cosine formula Eq. (11). Circles, 16 panels; triangles, 32 panels; squares, 64 panels.

Error Estimation

A unique feature of our method, made possible by the continuity of its results for the velocity distribution, is a capacity for checking its own accuracy a posteriori. As noted above, the only approximation made in the analysis is the assumption that the velocity distribution is linear on the panels. Once the nodal tangential velocities V_{t_i} are calculated, Eq. (5) can be adapted to calculate the velocity induced by the panels and the onset flow at the middle of the ith panel, $\hat{V}_i$. Then the nonlinearity of the velocity distribution on the ith panel is measured by

$$\Delta V_i \equiv \hat{V}_i - \tfrac{1}{2}(V_i + V_{i+1}) \tag{7}$$

in which V_i, V_{i+1} are the (now known) velocities at the end points of the ith panel.

Now the contribution of any panel to any quantity of interest (the potential or velocity, for example) at any field point is calculated by integrating over the panel the products of the source and vortex strengths with appropriate kernel functions, or, what is the same thing, the dot product of the velocity distribution on the panel with some vector kernel $\boldsymbol{K}$. The error incurred in this calculation due to the nonlinearity of the velocity distribution on the panel is, therefore,

$$\int_{i\text{th panel}} \Delta \boldsymbol{V}_i \cdot \boldsymbol{K} ds \sim \ell_i \Delta V_i \tag{8}$$

where ℓ_i is the length of the ith panel. This product, $\ell_i \Delta V_i$, is called the panel error function. Again, note that it can be calculated for each panel a posteriori, once the V_{t_i} have been determined, whether or not the exact solution is known.

From calculations of flows past ellipses, Joukowski airfoils, and Karman-Trefftz airfoils, using various numbers and distributions of nodes, we found the root-mean-squared error in the pressure coefficients at the nodes to correlate fairly well with the maximum value of the panel error functions. This suggested a node redistribution algorithm, in which a solution is obtained with a given set of nodes, which are then relocated so as to even out variations of the panel error function and so to reduce the maximum panel error. Since the nonlinearity of the velocity distribution on the ith panel is of order ℓ_i^2,

$$\ell_i \Delta V_i = O(\ell_i^3) \tag{9}$$

Thus we stretch the panels so that their new lengths ℓ_i' are given by

$$\ell_i' = c\ell_i / \sqrt[3]{\ell_i \Delta V_i} \tag{10}$$

in which c is chosen so as to fix the locations of the starting and ending points of the group of nodes being redistributed.§

Results obtained with this node redistribution algorithm for symmetric flow past an ellipse of thickness ratio ⅛ are shown in Fig. 4. For three different numbers of panels (16, 32, and 64) the nodes were initially distributed according to a cosine law

$$x_i = \cos\frac{\pi(i-1)}{N-1} \quad \text{for } i=1,\ldots,N \tag{11}$$

The root-mean-squared errors in C_p at the nodes observed in successive redistributions of the nodes are shown connected by solid lines.

In every case shown in Fig. 4, the redistribution algorithm reduced the maximum panel error; i.e., the history of the algorithm goes from right to left in Fig. 4. Usually it also reduced the rms error in the nodal C_p, although, given the order-of-magnitude basis of the algorithm, it would be too much to expect such a reduction every time. Indeed, the initial result in the 16-panel case was somewhat better than the final results, at least according to the measure of rms error in C_p at the nodes. However, with higher numbers of nodes, the algorithm improved the nodal C_p by factors of 3-5. (At least part of the worsening of the rms error with redistribution of 16 nodes is due to the fact that the initial distribution did not concentrate so many points near the stagnation points, where C_p is more rapidly varying.)

Because the algorithm cannot be guaranteed to optimize the node distribution, its efficient utilization required some experimentation. Since the objective is to reduce the maximum panel error by smoothing out variations in the panel error from one panel to another, the redistribution process is generally terminated when the ratio of the maximum panel error to the minimum is less than some fixed number on every network. Our experience shows little improvement in the solutions when this max/min ratio is reduced below about 4.0. This is illustrated in Fig. 4, in which the iterations were pursued in the 32-panel case until the max/min ratio was under 1.2. Points for which the ratio was under 4.0 are flagged. Note that the iterations do appear to be converging (though not necessarily to an "optimum" solution so far as the rms error in nodal C_p is concerned). This has been the case in all our calculations, at least when we use, as a

§Such a group of nodes, with fixed starting and ending points, is called a *network* in what follows. For example, separate networks are used for a wing's upper and lower surfaces, with their leading and trailing edges being fixed in the node redistribution process.

closure condition, stagnation conditions within the panels. An alternative approach, in which the closure condition was that the velocity inside the panels equaled that of the onset flow (so that the source and vortex strengths were components of the perturbation velocity normal and tangential to the panels), yielded divergent results for the case that is the subject of Fig. 4.

To avoid oscillations which otherwise were found in some cases, the node movement is under-relaxed by a constant factor when and if necessary to avoid an increase in the average node movement from one trial to the next. Even so, as will be seen later, we occasionally find that the maximum panel error increases with node redistribution. This usually indicates that further redistribution would not improve the solution significantly. Therefore, if the maximum panel error increases, we terminate the redistribution process and reject the distribution which yields the higher panel error.

Calculations similar to those reported in Fig. 4 were performed in which the initial node distribution was random. The histories of the rms error were quite similar to those shown in Fig. 4, except that the initial errors were much higher. In three trials with different initial distributions of 32 nodes, the rms error in the nodal C_p decreased during the node redistribution process from 0.3-0.4 to about 0.04.

While the final results obtained with the node redistribution algorithm are usually quite acceptable, the very magnitude of the improvement it brings is evidence that the subsurface panel method is extremely sensitive to the node distribution. This is brought home still more graphically by Fig. 5, which shows the history of the pressure distributions calculated at various stages of the node redistribution process. In that case, the ellipse initially exhibited a lift coefficient of about 1.5!

Studies of flows past a variety of other airfoils—including NACA four-digit airfoils and other formula-generated sections as well as Karman-Trefftz airfoils of varying thickness, camber, and trailing-edge angle—confirm the implications of Figs. 4 and 5, both as to the sensitivity of the subsurface panel method to the node distribution and the effectiveness of the node redistribution algorithm. The troubles of the basic method are not restricted to initially random distributions. The results of Figs. 6 and 7 were obtained starting with the "reasonable" distribution of Eq. (11). The implausible crossing over of the pressure distribution near the trailing edge shown in Fig. 6 is seen in Fig. 7 to lead to a 25% deficiency in the calculated lift coefficient, even when 64 panels are used. A possibly related anomaly was encountered near the sharp-but-not-cusped trailing edge of the highly cambered Karman-Trefftz airfoil to which Fig. 8 refers. In both cases, the anomaly was eliminated after a single application of the node redistribution algorithm.

Our final example, a multi-element airfoil, is displayed in Fig. 9 to demonstrate the prowess of the program used to implement the method.

Discussion and Conclusions

The effect of node distribution on results is not often discussed in the literature. Hess[1] gives a few results which indicate the effect can sometimes be substantial, but not nearly to the extent observed in the present study. From private communication with several of the authors of the present paper's references, and some limited experiments of our own with the classical constant-singularity-strength flat-panel method,[4] the subsurface panel method seems to be unusually sensitive to node distribution.

The cause of our oversensitivity to node distribution is not known. It is not the case, as has been suggested, that we are not satisfying the Kutta condition; the velocities we calculate are properly directed near the trailing edge. Nor does it seem to have to do with the $O(s\ln s)$ behavior of the velocity near the nodes. Similar results were obtained when we used cubic distributions of sources and vortices to reduce the singularity

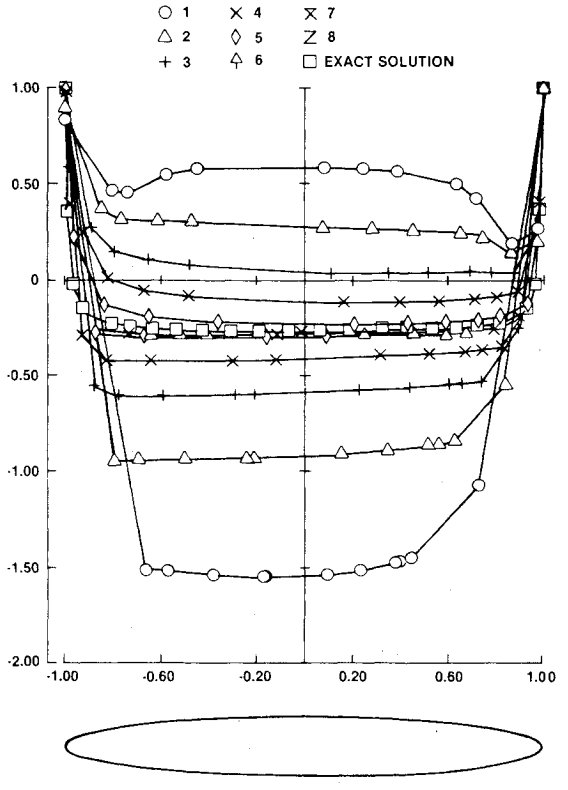

Fig. 5 Pressure distributions in successive stages of node redistribution process for ellipse of thickness ratio 0.125, starting with random distribution, 24 panels. Numbers indicate successive solutions.

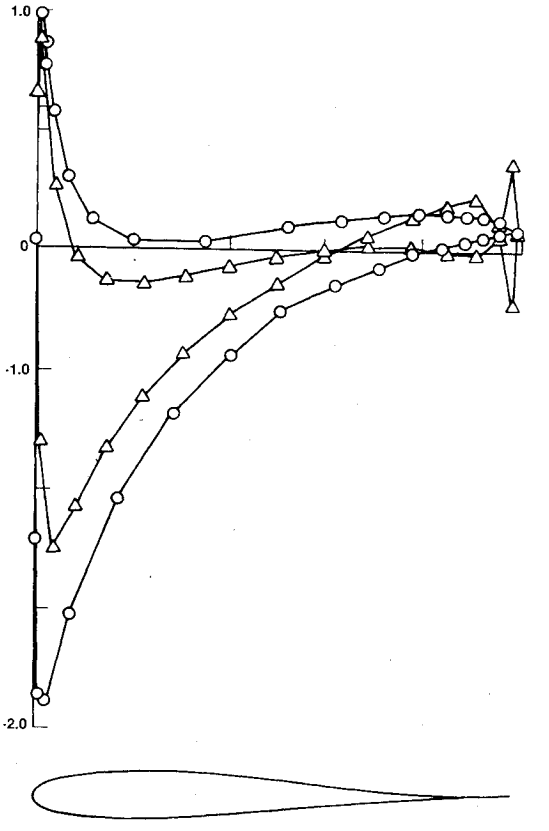

Fig. 6 Pressure distributions on simple uncambered airfoil with thickness proportional to $\sqrt{x}(1-x)^2$, angle of attack = 5 deg. Triangles obtained with cosine node distribution, circles after 4 node redistributions, 32 panels.

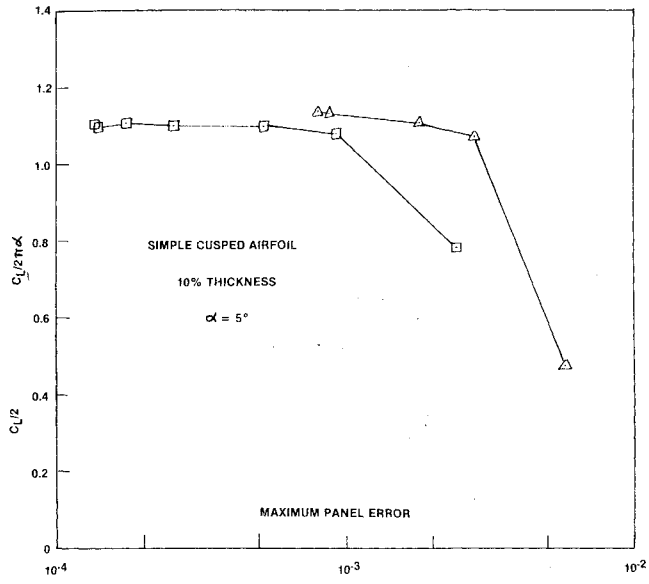

Fig. 7 History of lift coefficient during node redistribution process for airfoil of Fig. 6. Nodes initially distributed by cosine formula Eq. (11). Triangles, 32 panels; squares, 64 panels.

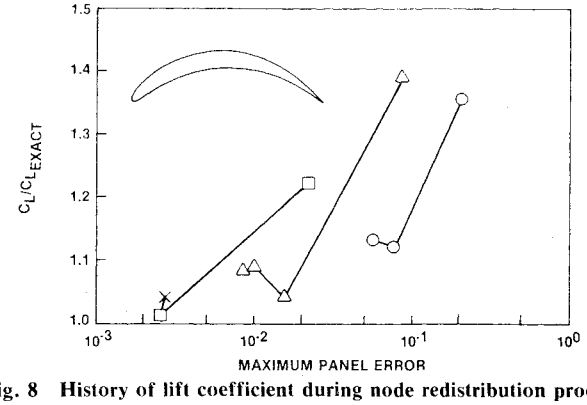

Fig. 8 History of lift coefficient during node redistribution process for highly cambered Karman-Trefftz airfoil (22% camber, 10% thickness) at zero angle of attack. Nodes initially distributed by equally spacing angular variable in circle plane. Circles, 16 panels; triangles, 32 panels; squares, 64 panels.

to $O(s^2 \ell n s)$ and to make dV_n/ds vanish at the nodes (along with V_n itself). On the other hand, if we compute, a posteriori, the velocity induced by the panels at points along the body surface, we find that our worst solutions are characterized by a large amount of leakage.

In order to eliminate this problem, we tried to control the normal velocity component in a way that would account for the velocity induced by all the panels rather than just the local flow-tangency condition. Simply replacing Eq. (5) by one which would set the panel-induced normal velocity component to zero leads, as is fairly well known, to an ill-conditioned matrix and to oscillations in the velocity from node to node. Similar results were obtained when we sought to minimize, with respect to the tangential velocity components V_{t_i}, the integral along the inside of the panels of either the square of the velocity component normal to the panels or the square of the magnitude of the velocity. An attempt to make the potential constant inside the panels also led to an ill-conditioned matrix. As would be expected our parameterizing the source and vortex strengths with derivatives of the potential diminished the diagonal dominance of the matrix, enough to give oscillatory answers. Less well understood are the failures of the results to improve when the equation set was amplified by the addition of requirements that the net

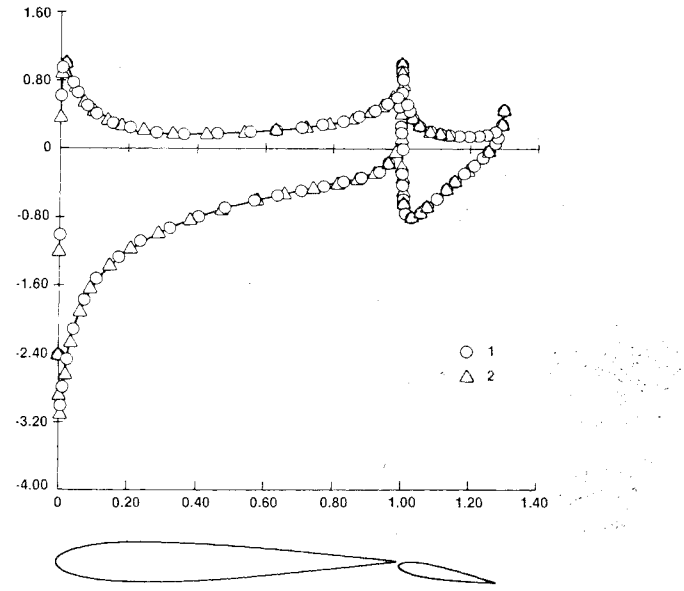

Fig. 9 Pressure distributions on two-element airfoil consisting of NACA 0012 sections: nose of flap 1% of wing chord below wing trailing edge; flap chord 30% of wing chord; flap deflection 10 deg, angle of attack 3 deg. Numbers indicate successive stages of redistribution process.

source strength vanish, or that the integral of $\partial\phi/\partial n$ along the inside of the body surface vanish (which is required to make the solution of the internal problem unique when its boundary condition is that the tangential velocity vanish on the inside of the body surface).

Late in the course of the research reported herein, it was recognized that the parameterization of the source and vortex strengths in terms of the nodal velocity components as described by Eqs. (2-4) was not unique in so far as obtaining a continuous velocity field is concerned. As noted in the Appendix, the V_{n_j} and V_{t_j} in Eq. (3) can be replaced by arbitrary functions of the node indices without altering our conclusions so far as continuity is concerned. In particular, we can devise a continuous version of the Douglas-Neumann method[4] by replacing the V_{t_j} by say, a constant Γ and the V_{n_j} by variables S_j, and determining those unknowns so as to make the panel-induced normal velocity component cancel the normal component of the onset flow at every node, and to satisfy a Kutta condition (such as equality of tangential velocity components at the trailing edge). The results we obtained with this method were even worse than those reported herein possibly because of reduced diagonal dominance in the coefficient matrix. As shown in the Appendix, the diagonal coefficient of the matrix associated with Eq. (5) (the coefficient of V_{t_i}) is

$$-1+1/2\pi(\nu_{i-1}+\nu_i)$$

in which $(\nu_{i-1}+\nu_i)$ is the angle subtended at the ith node by the $(i-1)$th and $(i+1)$th nodes, an angle that is generally less than π, much less so at the leading- and trailing-edge nodes. In our subsurface version of the Douglas method, the corresponding coefficient is simply

$$(\nu_{i-1}+\nu_i)$$

which can be relatively small.

Kemp[5] has devised a panel method very similar to the present one, in that it yields a continuous body-surface velocity distribution. His "loading vector" is essentially the nodal tangential velocity V_{t_i} of the present method, and he sets the nodal normal velocity component V_{n_i} in accordance with the local flow tangency condition, as do we. A major

difference is that Kemp determines the V_{t_i} so that the velocity induced by the panels is normal to the panels at their midpoints. Following publication of his report, we performed some limited experiments with Kemp's method. For symmetric flows past ellipses, we found it considerably more accurate than the present method. However, it seems to share our sensitivity to node distribution, yielding spurious results when the nodes were distributed randomly on the ellipse, and for an airfoil with a cusped trailing edge. Our node redistribution algorithm did not help in such cases. Of course, it could be that our implementation of Kemp's method was in error. In any case, satisfaction of boundary conditions at panel midpoints, while no problem in two dimensions, complicates the treatment of three-dimensional problems. As will be discussed in the epilogue which follows, use of the nodes as the sole control points leads to a very attractive singularity spline.

It is hoped that the evidence presented on the utility of the node redistribution scheme is convincing. In every case we have tried, it has enabled us to overcome the sensitivity of the method to the starting node distribution. Except when we play with random distributions, five or fewer iterations are sufficient to reach our criteria for terminating the redistribution process. Of course, this means that the method may require as much as six times the computation time of other methods for the same number of nodes, without any improvement in accuracy relative to higher-order methods like those of Hess,[1] Johnson and Rubbert,[2] and Bristow.[3] Therefore, the method is of practical interest only as a prototype of a method for three-dimensional flows.

Epilog

Whatever their worth for two-dimensional flows, panel methods are much more interesting in three-dimensional situations, where their ability to treat complicated geometries far exceeds that of currently available field methods. A three-dimensional version of the subsurface panel method described herein would enhance these advantages considerably. We have such a version in the debugging stage and enumerate here some of its features, since it may be of interest to know how much of the existing two-dimensional analysis which is the subject of this paper can be carried over to the three-dimensional case.

The method is based on distributions of sources and vortices (see Ward[6] for the basic equation) on plane triangular panels whose vertices are nodes on the body surface. Their strengths are components of the total fluid velocity on the outside of the panels and are assumed to vary linearly over the panels. The parameters of the source and vortex strengths are then the three components of the body-surface velocity distribution at the nodes which are vertices of the panel.

Since the velocity component normal to the body surface is known, we have two unknown singularity-strength parameters per node. For a given set of nodes, this gives us about twice as many unknowns as would be dealt with by other panel methods. This disadvantage may be overcome by the extremely local nature of our singularity splines; on any panel, our source and vortex strengths depend only on parameters associated with the vertices of that panel. Thus, as noted earlier, our effective mesh size may be considerably smaller than that of another panel method which uses the same node distribution.

The use of triangular panels greatly simplifies the geometry problem. All we must know about the body are its coordinates and the direction of its surface normal at each node. No approximation need be made for the body shape between nodes, even in calculating forces and moments. To be sure, we do require continuity of the body surface velocity, which excludes from current consideration flows past wings of zero thickness and other idealized problems.

The method yields a continuous body-surface velocity distribution. This will allow an estimate of the deviation from linearity of the velocity distribution on the panels, just as in the two-dimensional case. At this point, we do not know what would be the optimal way to use such information to improve the node distribution, but that remains well within the realm of possibility. For example, we could use the present algorithm directly to redistribute the nodes in a given row and/or column. If the number of iterations required to circumvent the sensitivity of this method to node distribution, which must be assumed to be as bad in the two-dimensional case, can be kept to the five or fewer required in the two-dimensional case, the simplification of the singularity splines and elimination of the geometry problem should make the subsurface approach quite competitive in three-dimensional situations.

Appendix

Let $V_j(x,y;\theta)$ be the contribution of the jth panel to the component of velocity in the direction θ at $P(x,y)$. To evaluate V_j, it is helpful to introduce local coordinates oriented with the jth panel:

$$x^* = (x-x_j)\cos\beta_j + (y-y_j)\sin\beta_j$$

$$y^* = (y-y_j)\cos\beta_j - (x-x_j)\sin\beta_j \tag{A1}$$

Then, if u^* and v^* are the velocity components at P along the (x^*, y^*) axes,

$$V_j = u^*\cos(\theta-\beta_j) + v^*\sin(\theta-\beta_j) \tag{A2}$$

Differentiating Eq. (1) and taking the source and vortex strengths to follow the linear laws of Eqs. (2), we find

$$\begin{bmatrix} u^*(x^*,y^*) \\ v^*(x^*,y^*) \end{bmatrix} = \begin{bmatrix} u_0 & v_0 & u_1 & v_1 \\ v_0 & -u_0 & v_1 & -u_1 \end{bmatrix} \begin{bmatrix} \sigma_0 \\ \gamma_0 \\ \sigma_\ell \\ \gamma_\ell \end{bmatrix} \tag{A3}$$

where

$$u_0(x^*,y^*) = \frac{1}{2\pi} - \left(1-\frac{x^*}{\ell_j}\right) f_\ell - \frac{y^*}{\ell_j} f_t$$

$$u_1(x^*,y^*) = \frac{1}{2\pi} - \frac{x^*}{\ell_j} f_\ell + \frac{y^*}{\ell_j} f_t$$

$$v_0(x^*,y^*) = \left(1-\frac{x^*}{\ell_j}\right) f_t - \frac{y^*}{\ell_j} f_\ell$$

$$v_1(x^*,y^*) = \frac{x^*}{\ell_j} f_t + \frac{y^*}{\ell_j} f_\ell \tag{A4}$$

and

$$f_\ell = (1/2\pi)\ln(r_{j+1}/r_j) \tag{A5}$$

$$f_t = (1/2\pi)\nu_j \tag{A6}$$

Here r_j is the distance from the jth node to $P(x,y)$ and ν_j is the angle subtended at P by the jth panel.

When P approaches either the jth or $(j+1)$th node, f_ℓ blows up and f_t depends on the direction of approach. However, if we consider the jth and $(j-1)$th panels in combination, then, near the jth node, we find

$$2\pi(V_{j-1}+V_j) = \ln r_j \{\sigma_{0_j}\cos(\theta-\beta_j) - \sigma_{\ell_{j-1}}\cos(\theta-\beta_{j-1}) - \gamma_{0_j}\sin(\theta-\beta_j) + \gamma_{\ell_{j-1}}\sin(\theta-\beta_{j-1})\}$$

$$+\nu_j\{\gamma_{0_j}\cos(\theta-\beta_j)+\sigma_{0_j}\sin(\theta-\beta_j)\}$$

$$+\nu_{j-1}\{\gamma_{t_{j-1}}\cos(\theta-\beta_{j-1})+\sigma_{t_{j-1}}\sin(\theta-\beta_{j-1})\}$$

$$+\text{terms regular near the } j\text{th node} \qquad \text{(A7)}$$

Here subscripts j and $j-1$ have been put on the source and vortex strengths to indicate the panel with which they are associated; recall that the singularity strengths are not continuous from one panel to the next.

On substituting for the σ's and γ's in Eq. (A7) from Eq. (3), we find that the logarithmically singular terms cancel one another, while the remaining terms reduce to

$$V_{j-1}+V_j=1/2\pi(\nu_j+\nu_{j-1})[V_{n_j}\sin(\theta-\theta_j)+V_{t_j}\cos(\theta-\theta_j)]$$

$$+\text{terms regular near the } j\text{th node} \qquad \text{(A8)}$$

While ν_j and ν_{j-1} are indeterminate as P approaches the jth node, their sum approaches the angle subtended at the jth node by the $(j-1)$th and $(j+1)$th nodes. Thus the velocity due to the linear singularity distributions Eqs. (2), with parameters given by Eq. (3), is continuous on and outside the panels. Near the nodes, it has an $s\ell n s$-type behavior. It is easy to show that these same results would obtain if V_{n_i} and V_{t_i} in Eq. (3) were replaced (consistently) by arbitrary functions of the node indicator i.

To apply these results to Eq. (5), simply let θ in Eq. (A8) become θ_i. Then the integral in Eq. (5) becomes

$$1/2\pi(\nu_i+\nu_{i-1})V_{t_i}+\text{terms regular near the } i\text{th node}$$

Therefore, in forming the coefficient matrix which governs the nodal tangential velocity components, we simply set ℓnr_j and ν_j equal to zero whenever they threaten to become singular and indeterminate, respectively, and compensate by adding $(\nu_i+\nu_{i-1})/2\pi$ to the coefficient of V_{t_i}.

Acknowledgment

This research was supported in part by NASA Ames Research Center, under Grant NSF-2316. A large fraction of the work was completed while the first author was a guest of A. R. Seebass, first at the University of Arizona and then at the University of Washington. It was a pleasure to acknowledge many simulating conversations with Seebass and his colleagues, and also the additional support given the research during that phase of it by the Office of Naval Research, under Contract N00014-76-0182.

References

[1] Hess, J. L., "Higher Order Numerical Solutions of the Integral Equation for the Two-Dimensional Neumann Problem," *Computational Methods in Applied Mechanics and Engineering*, Vol. 2, 1973, pp. 1-15.

[2] Johnson, F. T. and Rubbert, P. E., "Advanced Panel-type Influence Coefficient Methods Applied to Subsonic Flows," AIAA Paper 75-50, 1975.

[3] Bristow, D. R., "Recent Improvements in Surface Singularity Methods for the Flowfield Analysis about Two-Dimensional Airfoils," AIAA Paper 77-641, 1977.

[4] Hess, J. L., "The Problem of Three-Dimensional Lifting Potential Flow and its Solution by Means of Surface Singularity Distribution," *Computational Methods in Applied Mechanics and Engineering*, Vol. 4, 1974, pp. 283-319.

[5] Kemp, W. B. Jr., "A Vector-Continuous Loading Concept for Aerodynamic Panel Methods," NASA TM 80104, 1979.

[6] Ward, G. N., *Linearized Theory of High-Speed Flow*, Cambridge University Press, 1955, pp. 40-42.